Title
Skp2 Depletion Reduces Tumor-Initiating Properties and Promotes Apoptosis in Synovial Sarcoma

Journal
Translational Oncology, 13(10)

ISSN
1944-7124

Authors
Wang, Jichuan
Sato, Kenji
O'Donnell, Ed
et al.

Publication Date
2020-10-01

DOI
10.1016/j.tranon.2020.100809

Peer reviewed

Translational Oncology 13 (2020) 100809

Contents lists available at ScienceDirect

Translational Oncology

journal homepage: www.elsevier.com/locate/tranon

Skp2 Depletion Reduces Tumor-Initiating Properties and Promotes Apoptosis in Synovial Sarcoma

Jichuan Wang [a,b], Kenji Sato [a], Ed O'Donnell [a], Amit Singla [a], Simon Yaguare [a], Osama Aldahamsheh [a], Brian Batko [a], Hasibagan Borjihan [a], Janet Tingling [a], Jinghang Zhang [c], Daniel A. Weiser [d], David M. Loeb [d], Richard Gorlick [e], Edward L. Schwartz [f], Rui Yang [a], Xiaolin Zi [g], Hongling Zhao [h], David S. Geller [a], Bang H. Hoang [a,*]

[a] Department of Orthopedic Surgery, Montefiore Medical Center, Albert Einstein College of Medicine, Bronx, NY
[b] Musculoskeletal Tumor Center, Beijing Key Laboratory for Musculoskeletal Tumors, Peking University People's Hospital, Beijing, China
[c] Flow Cytometry Core Facility, Albert Einstein College of Medicine, Bronx, NY
[d] Division of Pediatric Hematology-Oncology, Children's Hospital at Montefiore, Albert Einstein College of Medicine, Bronx, NY
[e] Division of Pediatrics, University of Texas MD Anderson Cancer Center, Houston, TX
[f] Departments of Medicine (Oncology) and Molecular Pharmacology, Albert Einstein College of Medicine, Bronx, NY
[g] Department of Urology, University of California, Irvine Medical Center, Orange, CA
[h] Department of Developmental and Molecular Biology, Albert Einstein College of Medicine, Bronx, NY

ARTICLE INFO

Article history:
Received 10 February 2020
Received in revised form 22 May 2020
Accepted 26 May 2020
Available online xxxx

ABSTRACT

Synovial sarcoma (SS) is an aggressive soft-tissue cancer with a poor prognosis and a propensity for local recurrence and distant metastasis. In this study, we investigated whether S phase kinase-associated protein (Skp2) plays an oncogenic role in tumor initiation, progression, and metastasis of SS. Our study revealed that Skp2 is frequently overexpressed in SS specimens and SS18-SSX transgenic mouse tumors, as well as correlated with clinical stages. Next, we identified that genetic depletion of Skp2 reduced mesenchymal and stemness markers, and inhibited the invasive and proliferative capacities of SS cell lines. Furthermore, Skp2 depletion markedly suppressed the growth of SS xenografts tumors. Treatment of SS cell lines with the skp2 inhibitor flavokawain A (FKA) reduced Skp2 expression in a dose-dependent manner and resulted in cell cycle arrest and apoptosis. FKA also suppressed the invasion and tumor-initiating properties in SS, similar to the effects of Skp2 knockdown. In addition, a combination of FKA and conventional chemotherapy showed a synergistic therapeutic efficacy. Taken together, our results suggest that Skp2 plays an essential role in the biology of SS by promoting the mesenchymal state and cancer stemness. Given that chemotherapy resistance is often associated with cancer stemness, strategies of combining Skp2 inhibitors with conventional chemotherapy in SS may be desirable.

Introduction

Synovial sarcoma (SS) is an aggressive soft-tissue malignancy that commonly affects adolescent children and young adults. Despite multimodality treatment involving surgery, chemotherapy, and radiation, patients still sustain a high rate of local recurrence and distant metastasis. More than 95% of SSs is characterized by the cytogenetic aberration t(X:18)(p11.2:q11.2), in which the oncogenic event is the fusion of the SS18 gene on chromosome 18 with SSX1, SSX2, or SSX4 on the X chromosome [1]. The role of SS18-SSX fusion products in the initiation and progression of SS is an active area of investigation. Despite years of investigation, efforts in generating therapeutic agents that target the fusion oncoproteins have not been successful [2–4].

Skp2 is an F-box protein and E3 ubiquitin ligase that participates in many cellular processes such as cell cycle control, apoptosis, and regulation of cancer stemness [5,6]. Skp2 serves as a substrate recognition component of the Skp1-Cullin1-F-box (SCF) complex, acting to ubiquitinate and degrade other proteins. Skp2 is often overexpressed in human cancers and associated with a poor prognosis. For example, higher levels of Skp2 in the prostate, gastric, and esophageal cancers are correlated with distant metastasis and reduced survival. Conversely, downregulation of Skp2 leads to inhibition of tumor growth and metastasis [5,7–10]. Using the GEO database and tissue microarrays, we recently reported that high levels of Skp2 predict a poor prognosis in osteosarcoma [10]. Depletion of Skp2 by genetic knockdown or by the neddylation inhibitor flavokawain A (FKA) effectively inhibits osteosarcoma invasion *in vitro* and lung metastasis *in vivo*. In SS,

* Address all correspondence to: Bang H. Hoang, Department of Orthopedic Surgery, Montefiore Medical Center, Albert Einstein College of Medicine, Bronx, NY.
E-mail address: bahoang@montefiore.org. (B.H. Hoang).

http://dx.doi.org/10.1016/j.tranon.2020.100809

however, the mechanistic interaction and therapeutic utility of Skp2 have not been explored.

Synovial sarcoma is considered a stem cell malignancy, resulting from a dysregulation of self-renewal and differentiation capacity driven by the SS18-SSX fusion protein [11]. Aldehyde dehydrogenase (ALDH) has been reported as a potential marker of stemness in SS [12]. As such, SS has been thought to contain distinct subpopulations of cells that possess tumor-initiating cell (TIC) properties, which may be responsible for tumorigenesis [13,14]. In addition, SS tumors have been found to overexpress Twist1, a transcription factor that plays essential roles in maintaining stemness in other mesenchymal stem cell (MSC)–related sarcomas [13,15–17]. Twist1 knockdown reduces the migratory and sphere-forming capacity of SS, suggesting that Twist1 is essential for SS stemness properties. In addition, the depletion of Twist1 suppresses the mesenchymal phenotype in SS and profoundly inhibits the growth of SS xenografts. Recently, the chemokine receptor CXCR4 was also found to be highly expressed in the sphere subpopulation of SS and exhibited stemness-associated markers [18]. Little is known, however, about other factors or mechanisms that regulate the TIC subpopulation in SS.

Recent studies have begun to explore the association between Skp2 and the induction of cancer stemness. The cell cycle regulator p27, an Skp2 target, was shown to regulate stem cell renewal and the epithelial-mesenchymal transition (EMT) by occupying the promoter of Twist1 and thereby controlling Twist gene expression in human embryonic stem cells [19]. In prostate cancer, Skp2 downregulation has been shown to reduce the $CD44^+CD24^-$ cell population, markers commonly used to identify prostate cancer TIC [20]. Mechanistically, Skp2 is thought to regulate the TIC phenotype in prostate cancer by stabilizing intracellular Twist1 via nondegradative ubiquitination [5]. In SS, however, the involvement of Skp2 in modulating TIC characteristics has not been examined.

In this study, we found that 1) Skp2 is overexpressed in SS cell lines and tumor tissues and 2) high expression levels are associated with advanced clinical stages. Based on these data and previous studies, we hypothesized that Skp2 plays a pro-oncogenic role that induces SS cells to proliferate, invade, and maintain cancer stemness. Depletion of Skp2 by short hairpin RNA (shRNA) or by pharmacological approaches led to the downregulation of Twist1, reduction of stemness markers, and upregulation of Skp2 targets. These cellular changes induced apoptosis and inhibited the proliferative capacity, cancer stemness, and the mesenchymal state of SS.

Materials and Methods

Cell Lines and FKA Preparation

Synovial sarcoma cell lines Hssy-II, Syo-I, Yamato, and Aska were maintained in Eagle's minimum essential medium supplemented with 10% fetal bovine serum. Human skeletal muscle cell (SKMC) (CC-2561) was purchased from Lonza (Lonza Walkersville, Inc., Walkersville, MD) and maintained with SkGM Skeletal Muscle Cell Growth Medium BulletKit (CC-3160). Human dermal fibroblast (HFB) (CC-2511) was purchased from Lonza (Lonza Walkersville, Inc.) and maintained with FGM-2 Fibroblast Growth Medium-2 BulletKit (CC-3132). Protocols from the manufacturer were followed during the culture process. All cells were maintained at 37°C in a humidified atmosphere containing 5% CO_2. Pure FKA (F4502) was obtained from LKT Laboratories, C1 compound (HY-16661) was obtained from MedChemExpress, and Z-VAD-FMK (FMK001) was obtained from R&D Systems. These reagents were dissolved in dimethyl sulfoxide (DMSO) and stored at −20°C.

Quantitative RT-PCR

Total RNA was isolated using the RNAeasy Mini Kit (Qiagen, Valencia, CA), and reverse transcription of total RNA was performed using the QuantiTect Reverse Transcription kit (Qiagen). Two-step quantitative PCR was performed using the QuantiTect SYBR Green PCR Kit (Qiagen). Real-time PCR was performed as previously described [10]. GAPDH was used as the internal control. GraphPad Prism version 8.0 was used to analyze results. The primer information was listed as Supplementary Table 1.

Tissue Microarray Immunohistochemistry

Synovial sarcoma tissue microarrays (TMAs) were purchased from US Biomax (US Biomax, Rockville, MD). Immunostaining for Skp2 protein was performed using an anti-Skp2 monoclonal antibody (Cell Signaling Technology, Danvers, MA). Briefly, tissue sections were deparaffinized with xylene, hydrated in alcohol, and immersed in Dako REAL peroxidase-blocking solution (DAKO Inc., Glostrup, Denmark). The sections were microwaved in 10 mM Tris buffer (pH 9.0) for 15 minutes, and then specific secondary antibody (Dako REAL EnVision/HRP) and detection reagent were applied. Stained tissues were scored according to the method of Shigemasa et al. [21]: When no nuclear-positive tumor cell stain could be identified or when focally distributed nuclear-positive tumor cells were less than 5%, the staining was considered negative. When more than 25% of the tumor cells showed positive nuclear staining, staining was considered positive. All cases were scored by four of the authors. In order to avoid bias, the clinical information was blinded to the observer.

Bioinformatics Analysis

Skp2 mRNA expression was compared with overall survival using The Cancer Genome Atlas (TCGA) sarcoma database, which was accessed from the cBioportal (http://www.cbioportal.org/). Median expression of Skp2 mRNA was used as a cutoff to distinguish low versus high levels of expression, and Kaplan-Meier analyses were performed. As of January 2019, we identified 255 matched cases whereby comparison of Skp2 mRNA expression and the relevant clinical information was possible. The Oncomine database (https://www.oncomine.org/) was retrieved for mRNA expression from human SS surgical resection samples. The NCBI GEO profiles (http://www.ncbi.nlm.nih.gov/geoprofiles) were inquired for the mRNA expression level of Skp2 In the SS18-SSX transgenic mouse model.

Skp2 Knockdown by Lentiviral shRNA

Skp2-specific shRNAs were designed by the shRNA Core Facility at Albert Einstein College of Medicine. The TRC Genome-Wide shRNA Collections for human were developed by The RNA Consortium. The GIPZ Lentiviral shRNAmir Libraries were developed by Open Biosystems (Thermo Scientific, Waltham, MA). Two shRNA sequences were as follows: shSkp2-1#: TCAAATTTAGTGCGACTTA, shSkp2-2#: CCAGTTGTCTATGA AGTAT. Empty pGIPZ vector was used as a control to shSkp2. Each shRNA lentiviral construct was generated using the pGIPZ vector. After virus transduction, cells were selected with 2 μg/ml puromycin. The knockdown efficiency of each construct was determined by Western blotting.

Western Blot Analysis

Cells were lysed in RIPA buffer (Cell Signaling Technology) with protease inhibitor (Cell Signaling Technology), and 30 μg of protein was extracted and separated electrophoretically on denaturing sodium dodecyl sulfate polyacrylamide gel, transferred to nitrocellulose membranes, blocked with 5% milk buffer, incubated with primary antibodies and appropriate secondary antibodies, and subsequently exposed to ECL reagents as previously described [10]. Antibodies against Skp2 (#2652), PARP (#9542s), cleaved PARP (#5625), ZO-1 (#8193), p27 Kip1 (#3686), caspase-7 (#9492), cleaved caspase-7(#8438), caspase-3 (#9662S), p21 Waf1/Cip1(# 2947), and E-cadherin (#14472) were purchased from Cell Signaling Technology. Antibodies against Twist1 (sc-81417), vimentin (sc-6260), N-cadherin (sc-8424), ETV4 (sc-113), ECT2 (sc-514750), and ALDH (sc-166362) were purchased from Santa Cruz (Santa Cruz, TX). Antibodies against Fbxw7(PAB9873) were purchased from Abnova (Walnut, CA).

Cell Invasion Assay

The cellular invasion was examined using the 24-well BioCoat Matrigel invasion chamber (Corning, NY) as previously described [10]. The percent of invading cells was normalized to cell viability for each FKA/C1 dose using the corresponding MTT assays. Normalized invading cells (%) = (# of invaded cells) / (initial no. of seeded cells) * (% viability at corresponding FKA/C1 dose). All experiments were performed in triplicates.

Sphere Formation Assay

A total of 4×10^4 cells were seeded in Cancer Stem Premium (ProMab, Inc., Richmond, CA) in the 96-well ultra-low attachment culture dish (Corning). Cultures were maintained by adding additional stem cell medium every 2 days. To evaluate the effects of FKA or C1, assays were performed by adding different concentrations of FKA or C1 to the initial culture medium, and the medium was replenished. The number of spheres in each well was counted on day 7, and photographs were captured by the EVOS Imaging System. All experiments were performed in triplicates.

ALDH Assay

The Aldefluor kit (Stem Cell Technologies, Vancouver, Canada) was used to identify cell populations with high ALDH enzymatic activity. FKA treatment was done 48 hours before the assays. A total of 1×10^6 cells were cultured and resuspended in Aldefluor assay buffer as recommended by the manufacturer. For negative control, Aldefluor-exposed cells were quenched with diethylaminobenzaldehyde (DEAB). After 50 minutes of incubation at 37°C, cells were analyzed by flow cytometry (BD Biosciences, San Jose, CA), and results were analyzed by Flow Jo 10.1. All experiments were performed in triplicates.

Cell Proliferation Assay

1-(4,5-Dimethylthiazol-2-yl)-3,5-diphenylformazan (MTT) assays (Sigma-Aldrich Co. LLC, St. Louis, MO) were performed as previously described [10]. For proliferation assays, 3 × 103 cells were plated into 96-well plates in 100 μl of growth medium. Cell proliferation was compared between SS cell lines transfected with control and Skp2-knockdown plasmids. For viability assays, cells were cultured in 96-well plates at a density of 3 × 103 cells in 100 μl of growth medium overnight. After treatment with FKA/C1 or 0.1% DMSO as a control for 24, 48, and 72 hours, MTT assays were performed. Dose-response curves were created using GraphPad Prism version 8.0 software to measure the relative viability (GraphPad, La Jolla, CA). All experiments were performed in triplicates.

Cell Cycle Analysis

FITC BrdU Flow Kit was purchased from BD Biosciences and used for cell cycle assays. After treatment with FKA or 0.1% DMSO for 48 hours, cells were harvested, BrdU labeled, stained, and assessed by flow cytometry (BD Biosciences), and results were analyzed by Flow Jo 10.1 as recommended by the manufacturer. All experiments were performed in triplicates.

Apoptosis Analysis

Annexin V-APC/7-AAD Apoptosis Kit was purchased from Abnova and used for apoptosis analysis. Cell apoptosis analysis was compared between SS cell lines transfected with scramble control versus Skp2-knockdown plasmids. Generally, cells were harvested, counted and washed by the binding buffer. The cells were stained with Annexin V-APC and 7-ADD, and assessed by flow cytometry (BD Biosciences) as recommended by the manufacturer. Results were analyzed by Flow Jo cytometry analysis software 10.1. All experiments were performed in triplicates.

Synergy Analysis of Drug Combination

CompuSyn software (version 2.0; ComboSyn, Inc., Paramus, NJ) was used to evaluate the synergistic effects of the combination of FKA and doxorubicin using the median-effect method [22]. MTT assays were performed to determine the fraction of cells affected (Fa). The combination index (CI) and dose-reduction index (DRI) were calculated using CompuSyn. In this analysis, the combined effect was reported as synergistic, antagonistic, or additive when the Log(CI) value was <0, >0, and 0, respectively. The drug dose-reduce inclination was reported as favorable dose reduction, not favorable dose reduction, or no dose reduction when the Log(DRI) value was >0, <0, and 0, respectively.

Xenograft Models

In Vivo Effects of Skp2 Knockdown

Animal experiments (#20180401) were approved by the Institutional Animal Care Utilization Committee (IACUC) of the Albert Einstein College of Medicine. Hssy-II cells transduced with scrambled control shRNA (Ctrl) or Skp2 shRNA (shSkp2) were implanted subcutaneously at 1.5×10^6 cells per animal ($N = 5$ animals per group). Cells were injected into the right flank in 0.15 ml of serum-free media and growth-factor–reduced Matrigel (1:1). Subcutaneous tumors were measured once weekly using an electronic caliper. To assess tumor volume, the greatest longitudinal diameter (length), and the greatest transverse diameter (width) were measured. Tumor volumes were calculated as previously described [10]. All animals were euthanized when any tumor reached the size limit according to our IACUC protocol. Tumor tissues were harvested, measured, and saved for further analysis.

In Vivo Effects of Neddylation Inhibitor of Skp2

A total of 2×10^6 Hssy-II cells were injected into the right flank SCID mice subcutaneously, and mice were divided into two groups randomly ($N = 6$ animals per group) and treated with vehicle, 0.5% w/v carboxymethyl cellulose (CMC), or FKA (600 mg/kg/day). Treatment was initiated 1 week after the injection of tumor cells. Tumors were measured once weekly using an electronic caliper, and all animals were euthanized when any tumor reached the size limit according to our IACUC protocol. Tumor tissues were harvested, measured, and saved for further analysis.

Statistical Analysis

The unpaired two-tailed Student *t* test was used for the analysis of qPCR expression, invasion assay, and sphere formation assay in the comparison between two groups. The chi-square test was performed in TMA analysis. The Dunnett's *t* test was used for invasion assay, sphere formation assay, and ALDH assay in the comparison between different concentrations of FKA. The two-way ANOVA was performed in proliferation and viability assay. These analyses were performed using GraphPad Prism and SPSS (version 22; SPSS, Chicago, IL). In the xenograft models, the difference between groups was assessed using the Mann-Whitney test. Statistical significance was set at $P < .05$.

Results

Skp2 Is Overexpressed in Synovial Sarcoma Patient Samples, Cell Lines, and Tumors from SS18-SSX Transgenic Mice, and High Expression Levels Are Associated with Advanced Clinical Stages

To assess Skp2 expression levels in SS, qRT-PCR was performed in established SS cell lines (SYO-I, Hssy-II, Yamato, Aska), patient-derived SS tumors (ST-039, ST-068, ST-086), normal MSCs, SKMC, and HFB (Figure 1*A*). Compared to MSC, SKMC, and HFB, Skp2 mRNA levels were elevated in ST-039 ($P < .001$), ST-068 ($P < .001$), ST-086 ($P < .001$), SYO-I ($P < .001$), Hssy-II ($P < .001$), Yamato ($P < .001$), and Aska ($P < .001$). Using the Oncomine database, we found that Skp2 mRNA expression

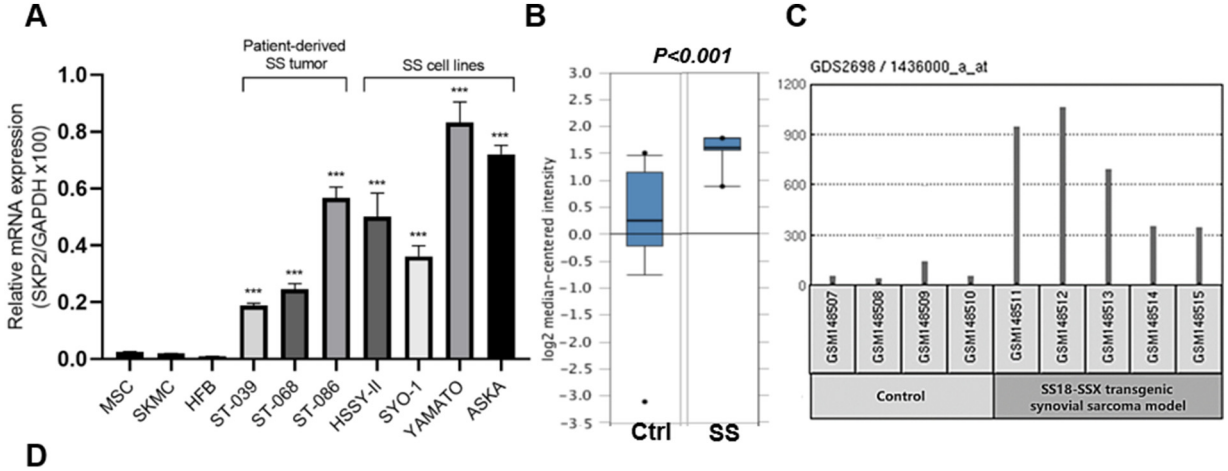

D

	Number	Skp2 positive staining (%)
Sex		
Male	30	53.3
Female	20	45.0
Age(yr)		
<40	24	58.3
>40	26	42.3
Stage		
I, II	25	44.0*
III, IV	25	56.0*

Figure 1. Skp2 is overexpressed in SS cell lines, patient samples, and transgenic mouse model. The high levels of skp2 correlate with worse clinical stages. (A) Relative mRNA expression of Skp2 in patient-derived (ST-039, ST-068, ST-086) and established SS cell lines (Hssy-II, Syo-1, Yamato, Aska) was significantly elevated compared to MSC, SKMC, and HFB, which served as controls. (B) Bioinformatics analysis of Skp2 mRNA expression in SS surgical resection samples ($n = 4$) compared to control samples ($n = 15$) and (C) transgenic synovial sarcoma mouse models compared to skeletal muscle controls using Oncomine database and NCBI GEO database. The mRNA level of Skp2 was markedly increased in SS patients samples and the SS18-SSX transgenic synovial sarcoma model ($P < .001$). (D) Immunohistochemical analysis of tissue microarrays was performed in 50 synovial sarcoma patients (US Biomax, SS1001). High levels of Skp2 protein expression were correlated with worse clinical stages (*$P = .045$). Statistical significance is indicated by *$P < .05$,**$P < .01$, ***$P < .001$. Column: mean; error bars: SD.

in human SS surgical resected specimens ($n = 4$) was significantly elevated compared to that in normal tissues ($n = 15$) ($P < .001$) (Figure 1*B*). In addition, our search of the NCBI GEO profiles also revealed that Skp2 expression in the SS18-SSX transgenic synovial sarcoma mouse tumors was markedly increased compared to that of control skeletal muscle samples (Figure 1*C*). Interestingly, an analysis of Skp2 mRNA expression in using TCGA of soft-tissue sarcoma also revealed that patients with higher expression of Skp2 exhibited a significantly more reduced overall survival ($P = .0248$, Supplementary Figure 1).

To further evaluate the clinical significance of Skp2 in SS, immunohistochemistry was performed using clinically annotated tissue microarrays (TMA, US Biomax, SS1001). The staining intensity was scored according to the method of Shigemasa et al. [21]. No statistically significant difference in the mean percentage of cells stained positively for Skp2 was found between different gender or age groups. However, the mean percentage of cells stained positively for Skp2 was higher in clinical stage III-IV cases compared to clinical stage I-II cases ($P = .045$) (Figure 1*D*) (Supplementary Figure 2), suggesting that high levels of Skp2 are associated with SS progression.

Skp2 Is Essential for Synovial Sarcoma Proliferation, Invasion, and Tumor-Initiating Properties

Since our expression analysis suggests that Skp2 plays a pro-oncogenic role in SS, we next knocked down Skp2 by shRNA to determine its biological significance. The efficiency of Skp2 knockdown was confirmed by Western blots (Figure 2*C*, Supplementary Figure 3). In MTT assays, the silencing of Skp2 significantly reduced the proliferative capacity of Hssy-II and Syo-1 cell lines ($P < .001$) (Figure 2*A*), along with a corresponding elevation of p21 and p27, known SCF-Skp2 substrates (Figure 2*C*). After Skp2 knockdown, Matrigel invasion assays showed 59.9% (2128 ± 1716 vs 5312 ± 1313, $P = .018$) and 41.6% (4742 ± 1348 vs 8121 ± 1426, $P = .021$) reduction in the invasion of Hssy-II and Syo-1 cell lines, respectively (Figure 2*B*). In addition, levels of cleaved PARP were elevated following Skp2 knockdown (Figure 2*C*), suggesting that depletion of SCF-Skp2 activity promotes apoptosis. Further apoptosis assays confirmed that Skp2 downregulation significantly increased apoptosis in both Hssy-II ($P = .032$) and Syo-I ($P = .023$) cell lines (Figure 2*D*). When scramble control and Skp2 knocked down Syo-I cells were treated with Z-VAD-FMK (a pan-caspase inhibitor), caspase-3 cleavage was partly blocked by Z-VAD-FMK (Supplementary Figure 4*B*), suggesting that Skp2 inhibition led to caspase-mediated apoptosis.

To determine the role of Skp2 in maintaining SS tumor-initiating properties, we examined levels of TIC biomarkers in Hssy-II and Syo-1 cell lines. First, we found that Skp2 knockdown led to a marked reduction in TIC markers such as EVT4 and ALDH by immunoblotting (Figure 2*C*), and CD44, CD133, and CD29 by qPCR (Supplementary Figure 5). Next, we assessed the effects of Skp2 knockdown on anchorage-independent sphere-forming capacity as a surrogate indicator of cancer stemness. The number of spheres formed by Hssy-II and Syo-I cell lines was reduced by 62.9% (10 ± 4 vs 27 ± 2, $P = .003$) and 63.6% (8 ± 2 vs 22 ± 7, $P = .029$), respectively, after Skp2 knockdown by shRNA (Figure 3*A*). We

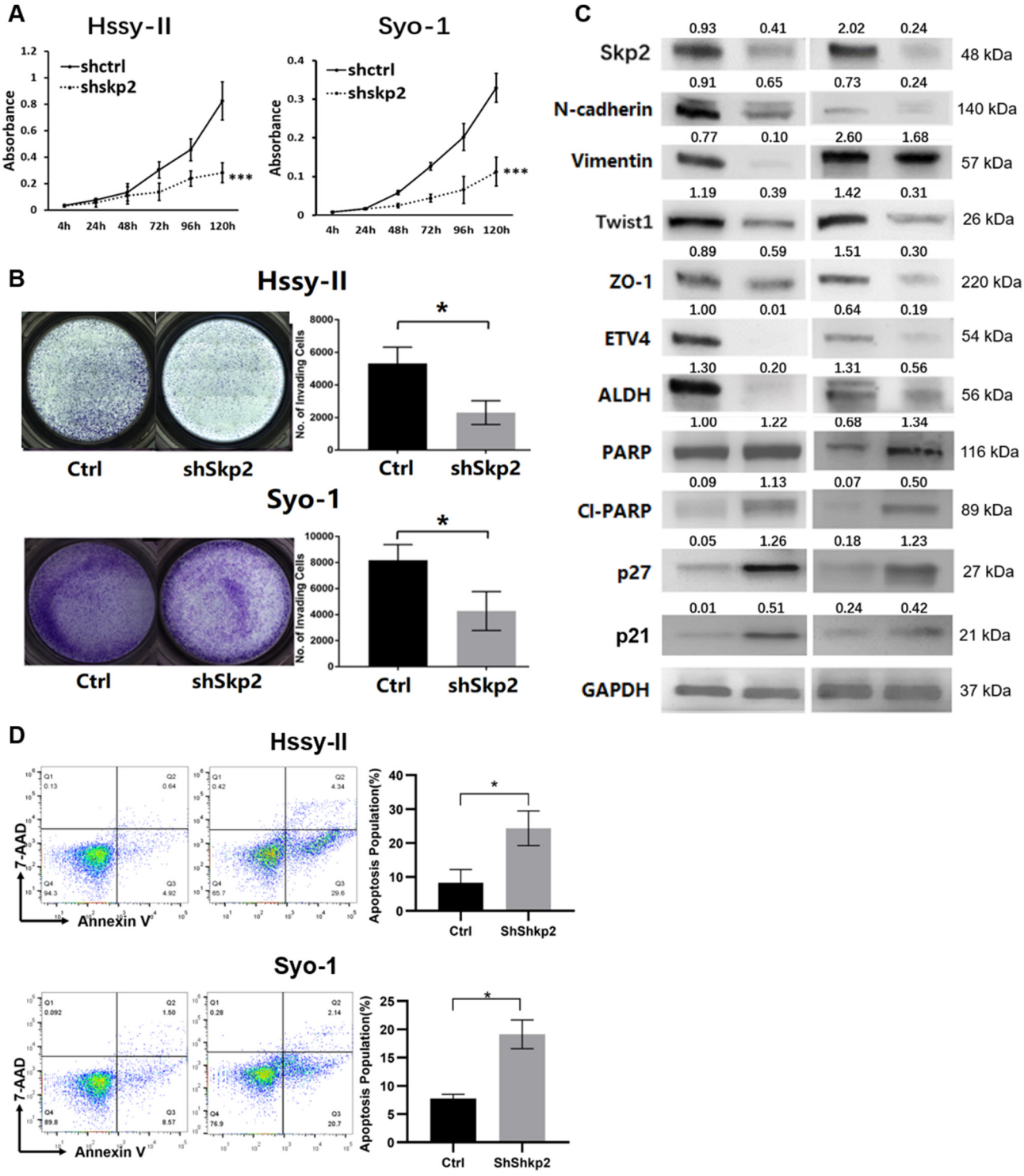

Figure 2. Proliferation, invasion, and biomarker studies following genetic knockdown of Skp2 in SS cell lines. (A) Cell proliferation assays. Compared to scramble transfected cells, the proliferation of shSkp2 Hssy-II and Syo-1 cell lines were significantly reduced. (B) Matrigel invasion assays. Representative pictures of invasion chambers were shown on the left, and statistical analysis was shown on the right. Compared to controls, invasion through Matrigel was significantly reduced in skp2 downregulation cells. (C) Western blot analysis. Downregulation of Skp2 was confirmed in Hssy-II and Syo-1 cell lines. After Skp2 knockdown, levels of Skp2 substrates (p21, p27), apoptotic markers (PARP, Cl-PARP), tumor initiation markers (Twist1, ALDH, ETV4, ZO-1) and mesenchymal markers (N-cadherin, Vimentin) were determined by immunoblotting. (D) Apoptosis induced by Skp2 knockdown was determined by FACS. Cells were stained with Annexin V and 7-AAD and analyzed by FACS for the identification of an apoptotic subpopulation. Representative FACS results were shown on the left, and statistical analysis was shown on the right. Statistical significance is indicated by $*P < .05$,$**P < .01$, $***P < .001$. Column: mean; error bars: SD.

further evaluated the effects of Skp2 depletion on TIC population by determining ALDH activity. As a control, SS cell lines were treated with DEAB, a specific ALDH inhibitor. We found that 0.86% of Hssy-II and 0.96% of Syo-1 were positive for ALDH, which served as the background control for gating strategy. After subtracting the background control, 14.74% of Hssy-II and 16.34% of Syo-1 cells were found to exhibit high ALDH activity and

defined as the ALDH-bright population (ALDHBr). After downregulation of Skp2, the ALDHBr fraction decreased from 14.74% to 1.58% in Hssy-II and 16.34% to 1.53% in Syo-1 cell lines. Further statistical analysis confirmed significant decrease in both Hssy-II ($P = .019$) and Syo-I ($P = .021$) cell lines, respectively (Figure 3*B*). Together, our data indicate that Skp2 depletion reduced the properties of TIC in SS.

Since our *in vitro* study suggests that Skp2 is essential for preventing apoptosis and maintenance of TIC population in SS, we evaluated the effects of Skp2 knockdown on tumorigenicity *in vivo*. For these experiments, Hssy-II cells transduced with lentivirus encoding shSkp2 or a scramble control were injected subcutaneously into SCID mice. As a result, knockdown of Skp2 significantly inhibited the growth of Hssy-II xenografts (Figure 3, *C* and *D*), and the relative final tumor volume of the Skp2 knockdown group (428.4 ± 157.9 mm^3) was significantly lower than that of the control group (2525.6 ± 243.1 mm^3) ($P = .008$, Figure 3*E*). Collectively, our results suggest that Skp2 has antiapoptotic, proinvasive activities and promotes tumor growth in SS xenografts. *In vitro* data strongly suggest that Skp2 participates in the maintenance of mesenchymal and tumor-initiating features of SS.

Pharmacologic Inhibition of Skp2 Reduces Synovial Sarcoma Proliferation, Invasion, and Stemness Properties

The Inhibition of Skp2 by Skp2 Inhibitors FKA or C1 Compound [23] Inhibits Synovial Sarcoma Cellular Proliferation and Invasion

To investigate the effects of Skp2 inhibitors on SS proliferation and invasion, we next treated Hssy-II and Syo-1 cell lines with FKA, a neddylation inhibitor for targeting Skp2 degradation [24], and performed viability

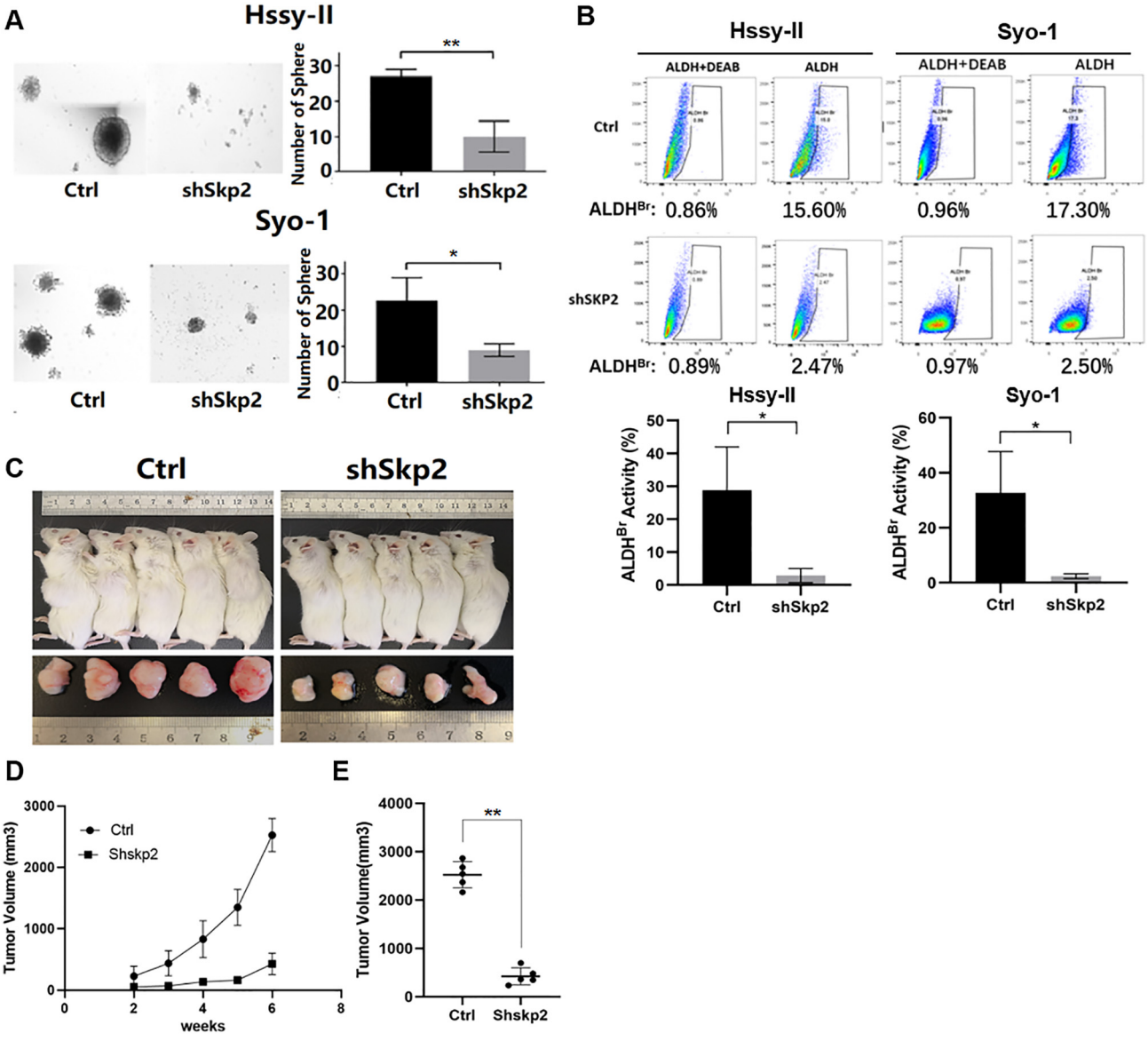

Figure 3. Sarcosphere formation, ALDH activity assay, and *in vivo* xenograft study following genetic downregulation (shSkp2) of Skp2 in SS cells. (A) Sarcosphere formation assays using Hssy-II and Syo-1 cell lines showed that the number of sarcospheres was markedly reduced by downregulation of Skp2. Representative pictures of the spheres were shown on the left, and statistical analysis was shown on the right. (B) ALDH activity of Hssy-II and Syo-1 cell lines was determined by FACS analysis. Representative FACS analysis results of scramble (Ctrl) or Skp2 knockdown (shSKP2) cell lines with and without DEAB (ALDH inhibitor) were shown. ALDH activity was decreased in shSkp2 group compared to the Ctrl group after eliminating the background (ALDH + DEAB) in both Hssy-II and Syo-1 cell lines. Statistical analysis was shown on the bottom. (C) Hssy-II cells were transduced with lentivirus expressing either scramble control shRNA (Ctrl) or Skp2 shRNA (shSkp2). Transduced cell lines were subcutaneously injected into the flank of SCID mice. Corresponding tumors from five independent xenografts were shown, and the relative tumor growth (D) and tumor volume at sacrifice were presented (E). The growth of shSkp2 tumors was significantly reduced compared to the control group. ($P = .008$). Statistical significance is indicated by $*P < .05$,$**P < .01$, $***P < .001$. Column: mean; error bars: SD.

assays. After 24 or 72 hours, FKA treatment led to a significant decrease in cell viability in SS cell lines but not in MSCs. At 10 μg/ml, FKA inhibited the growth of Hssy-II and Syo-1 cells by approximately 60%. Similar antiproliferative effects using C1, an SCFSkp2/Cks1 inhibitor, was confirmed by viability assays (Supplementary Figure 6*A*). Next, to evaluate the effects of FKA on cellular invasiveness, we performed Matrigel invasion assays on SS cell lines Hssy-II and Syo-1. The percent of invading cells was normalized to cell viability for each FKA dose using the corresponding MTT assay.

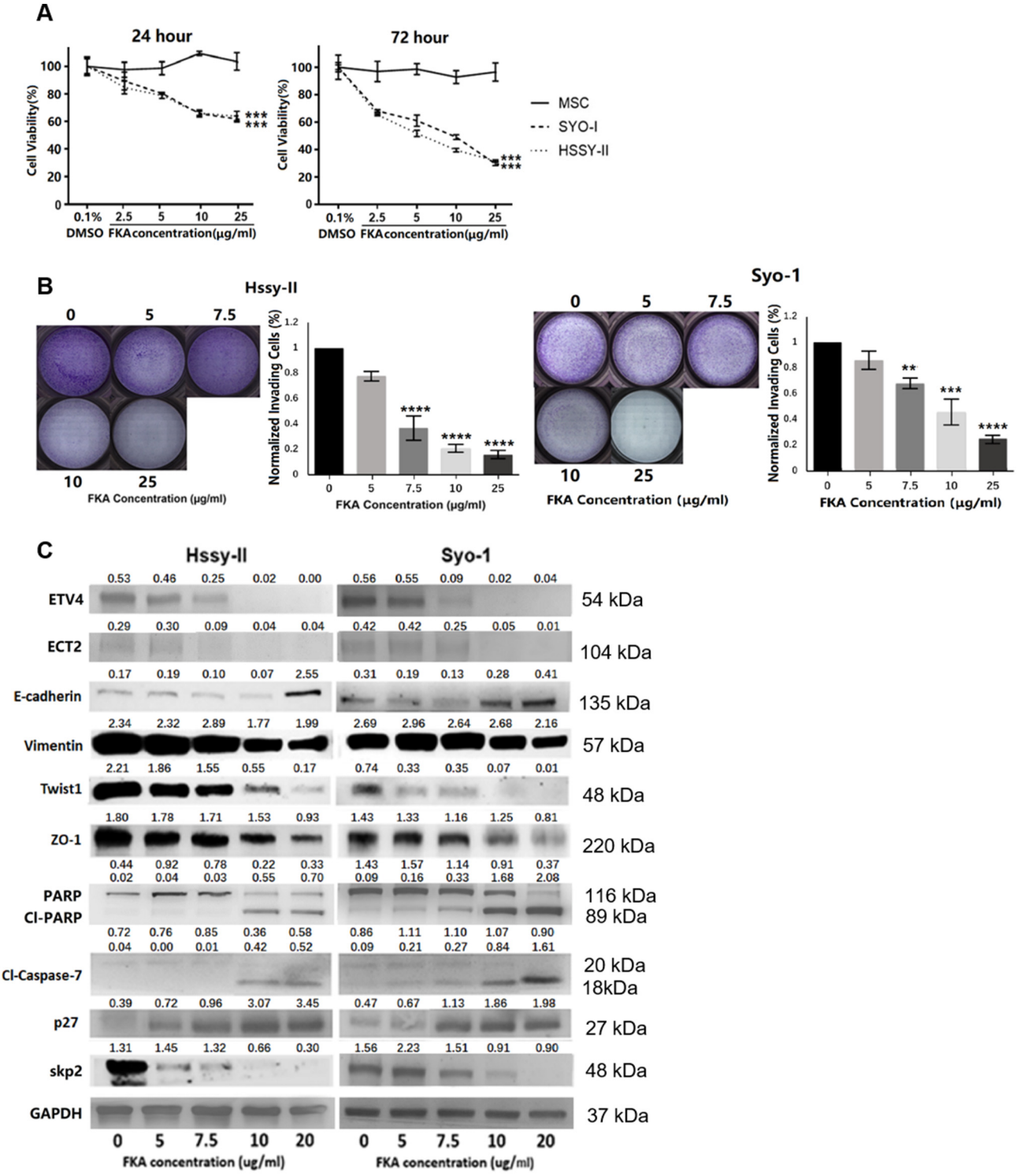

Figure 4. Proliferation, invasion and biomarker studies following inhibition of Skp2 by FKA in SS cells. (A) Hssy-II and Syo-1 cell lines were treated with serial dilutions of FKA for 24 and 72 hours, and cell viability was determined using MTT assays. Representative curves from three independent experiments are shown. Human MSCs were used as control. FKA inhibits cell viability in SS cell lines but not in MSC. Two-way ANOVA was used for statistical analysis. (B) Matrigel invasion assays. Representative pictures of invasion chambers were shown on the left, and statistical analysis was shown on the right. Results were normalized to the corresponding MTT assays. (C) Western blot showing FKA-mediated suppression of Skp2 in a dose-dependent manner. Levels of Skp2 substrate (p27), apoptotic markers (PARP, Cl-PARP, Cl-Caspase7), tumor stemness and initiation markers (Twist1, ECT2, ETV4, ZO-1), mesenchymal marker (Vimentin), and epithelial marker (E-cadherin) were determined by immunoblotting. Statistical significance is indicated by $^{*}P < .05$, $^{**}P < .01$, $^{***}P < .001$, $^{****}P < .0001$. Column: mean; error bars: SD.

Matrigel invasion assays showed that FKA significantly inhibited SS cellular invasion in a dose-dependent manner. Compared to controls, treatment with 10 μg/ml of FKA reduced cellular invasion by 76.2% in Hssy-II ($P < .0001$) and 54.3% in Syo-1 ($P = .0004$), while 25 μg/ml of FKA reduced cellular invasion by 84.5% in Hssy-II ($P < .0001$) and 74.3% in Syo-1 ($P < .0001$) (Figure 4*B*). Similarly, a significant decrease in invasion was also achieved with C1 (Supplementary Figure 6*C*) in both Hssy-II ($P = .0078$) and Syo-1 ($P = .0019$) cell lines.

Skp2 Inhibitors Induce Apoptosis and Cell Cycle Arrest

To determine the mechanisms underlying FKA-induced inhibition, we next treated SS cell lines with increasing concentrations of FKA and examined the effects on Skp2. Western blot analysis showed that FKA suppressed Skp2 expression in a dose-dependent manner (Figure 4*C*) without affecting the levels of fbxw7, another F-box protein family member (Supplementary Figure 7). Similar to the effects of Skp2 knockdown, FKA also induced an accumulation of p27, as well as apoptotic markers, including cleaved caspase-7 and cleaved PARP in Hssy-II and Syo-1 cells (Figure 4*C*). Western blot also showed C1-mediated suppression of Skp2 led to stabilization of p21 and p27 and an increase of apoptotic marker cleaved caspase-3 (Supplementary Figure 6*E*). When Syo-I cells were treated with FKA for 48 hours with or without Z-VAD-FMK (a pan-caspase inhibitor), caspase-3 cleavage was partly blocked by Z-VAD-FMK (Supplementary Figure 4*A*), indicating inhibition of apoptosis induced by FKA. To further investigate the effects of FKA on cell cycle regulation, 5-bromo-2′-deoxyuridine staining was performed. A significant dose-dependent decrease in S-phase cells and an increase in sub-G1 phase cells at 12.5 μg/ml and 25 μg/ml of FKA were found in Hssy-II and Syo-1 cell lines (Supplementary Figure 8). In Hssy-II, the percentage of S-phase cells in 12.5 μg/ml of FKA markedly decreased compared to vehicle control (15.7% vs 28.7%). In contrast, the sub-G1 fraction increased substantially after FKA treatment compared to vehicle control (27.7% vs 1.3%). In Syo-1 cells, the S-phase fraction decreased markedly after treatment with 12.5 μg/ml of FKA compared to vehicle control (25.5% vs 32.8%), while the sub-G1 fraction increased compared to vehicle control (12.1% vs 1.5%). Furthermore, a decrease in the G1-0 fraction was also found after FKA treatment in both cell lines. These results indicate that FKA likely induces G2/M cell cycle arrest and that apoptosis becomes more evident as FKA concentration was increased.

Skp2 Inhibitors Suppress Stemness in SS Cell Lines

Since FKA is a neddylation inhibitor that reduces Skp2 expression [24], we investigated whether FKA can modulate the tumor-initiating properties of SS cell lines. SS cell lines were treated with increasing concentrations of FKA, and Western analysis was performed. First, we found that transcriptional regulators Twist1 and ZO-1 were reduced after FKA treatment. Next, treatment with FKA resulted in a reduction in stemness markers ETV4s and ECT2 (Figure 4*C*). Additionally, we also examined sphere-forming capacity after FKA treatment in SS cell lines Hssy-II and Syo-1. After incubation of 7 days, both SS cell lines formed significantly fewer spheres in FKA treatment group than in the vehicle control group in a dose-dependent manner ($P < .001$ in Hssy-II, $P < .001$ in Syo-1; Figure 5*B*). Furthermore, we evaluated the effect of FKA on tumor-initiating cell indicators like ALDH activity. SS cell lines treated with FKA at the 10 μg/ml showed a significant decrease in ALDH activity compared to cell lines treated with vehicle control. The percentage of cells with high ALDH activity ($ALDH^{Br}$) was reduced from 29.4% to 1.87% in HSSY-II and 42.72% to 27.36% in Syo-1 cell lines after FKA treatment (Figure 5*A*). A further concentration gradient analysis showed a dose-dependent inhibition of ALDH activity in both cell lines (Figure 5*A*). Similar suppressive effects were observed by using the C1 compound (Supplementary Figure 6, *D* and *E*). Taken together, these data suggest that Skp2 inhibitor phenocopies Skp2 genetic knockdown in suppressing TIC properties in SS.

FKA Functions as an Skp2 Inhibitor and Acts Synergistically with Doxorubicin. Since FKA suppresses stemness markers in SS cell lines, we tested whether FKA can function synergistically with doxorubicin, a chemotherapeutic agent commonly used in SS. The cell viability after treatment with a single agent or a combination was determined by MTT assays. The synergistic effect of the drug combination is determined by the median-effect method [22]. Based on the CI result, the combination of FKA and doxorubicin showed strong synergistic tendencies in both Hssy-II and Syo-1 cell lines (Supplementary Figure 9*A*). In a dose-reduction analysis, the addition of FKA with doxorubicin was favorable in further reducing the dosage of doxorubicin in both Hssy-II and Syo-1 cell lines (Supplementary Figure 9*B*). Together, these results suggest that FKA and doxorubicin display a potent synergistic efficacy, and therefore, a strategy of combining Skp2 inhibitors with conventional chemotherapy in SS may be desirable.

Oral FKA Treatment Reduces Tumor Growth in SS Xenografts

Since our *in vitro* studies suggest that FKA promotes apoptosis and inhibits TIC properties, we proceeded to examine the effects of FKA *in vivo* using an SS xenograft model. We selected 600 mg/kg of FKA since this dosage has been shown previously to induce apoptosis in an osteosarcoma xenograft model [10]. FKA was administered daily by oral gavage 1 week after successful engraftment of Hssy-II subcutaneous xenografts. After 6 weeks of treatment, the average growth of tumor volumes of the PDX models is slower in the FKA treatment group (Figure 5*C*). The mean tumor volumes were significantly reduced in the FKA-treated group ($1230.6 \pm 531.8\ mm^3$) compared to the vehicle control group (0.5% w/v CMC) ($2225.6 \pm 502.3\ mm^3$) ($P = .026$; Figure 5*D*). Body weight did not differ significantly between the treated and control groups during the treatment period (data not shown). Taken together, FKA-mediated tumor-suppressive effects were validated with our *in vivo* model.

Discussion

In the present study, we have identified the F-box protein Skp2 as a proto-oncogene in SS, which is overexpressed in SS cell lines, surgical specimens, and SS18-SSX fusion-driven mouse tumors. As such, SS tumors express higher levels of Skp2 protein in more advanced clinical stages. Furthermore, our study demonstrates that both genetic and pharmacologic suppression of Skp2 inhibits SS cellular proliferation, invasion, and TIC properties, leading to apoptosis and cell cycle arrest. *In vivo*, Skp2 knockdown is associated with significant growth-inhibitory effects in an SS xenograft model. Given the paucity of studies on mechanisms of TIC in SS, our results demonstrate that Skp2 likely promotes stemness by modulating the CDK inhibitor p27 and the mesenchymal marker Twist1.

Although Naka and colleagues [11] reported that TICs exist in SS, the molecular mechanisms supporting this cell population are still unclear. Twist1 is a basic helix-loop-helix transcription factor that plays critical roles in tissue development and cancer progression and metastasis [16,25]. Recently, a study by Lee et al. [13] has linked Twist1 to TIC characteristics in SS cell lines, and deficiency in Twist1 inhibits the growth of SS xenografts by promoting apoptosis and cell cycle arrest. More importantly, these investigators showed that Twist1 is likely a downstream effector of the SS18-SSX gene product and acts to maintain TIC properties in SS cells, such as ALDH activity and sphere-forming capacity [13]. Others have also linked Twist1 through its inactivation of p53 to tumorigenesis of other sarcomas such leiomyosarcoma and pediatric osteosarcoma [26]. In our study, Skp2 depletion is associated with a corresponding decrease in Twist1, suggesting that Skp2 is upstream and essential for Twist1 expression in SS cells. Recently, in castrate-resistant prostate cancer, Skp2 has been found to stabilize Twist1 protein by preventing β-TrCP–mediated Twist degradation [5]. As such, results from our study implicate that a high level of Skp2 in SS maintains Twist1 expression and thus enhances cancer stemness. Twist1 was reported to be influenced by the SS18-SSX fusion product [13]. More interestingly, we found that Skp2 levels were significantly upregulated after the introduction of the SS18-SSX transgene in mouse models. Together, these data raise the possibility that Skp2 may also participate in the SS18-SSX effector network and deserves further investigation.

Both Skp2 and its target p27 have been linked to stem cell properties in several systems. In the central nervous system, Skp2-mediated degradation

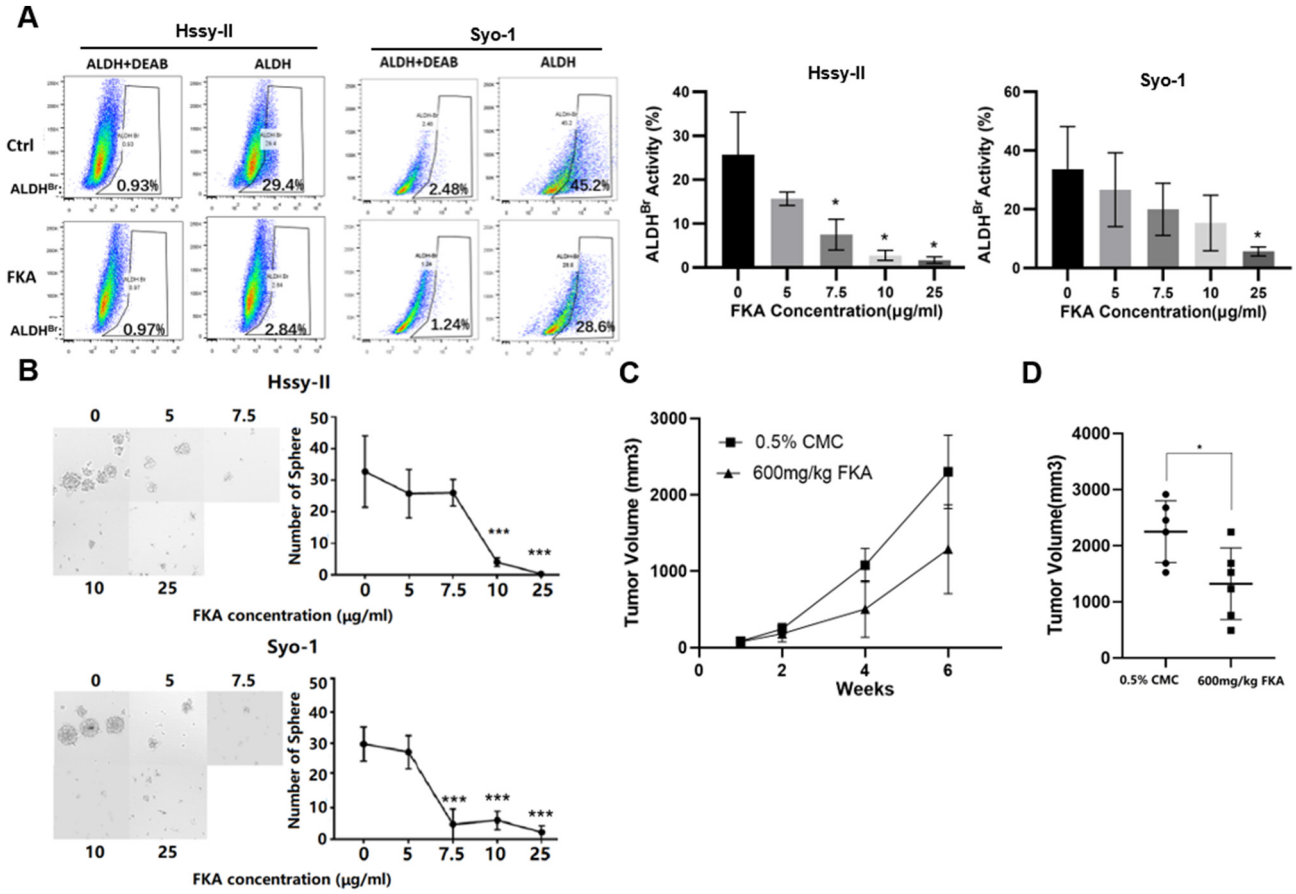

Figure 5. Inhibition of Skp2 by FKA suppresses synovial sarcoma ALDH activity, sarcosphere formation, and tumor growth *in vivo*. (A) ALDH activity of Hssy-II and Syo-1 cell lines was determined by FACS analysis. Representative FACS analysis results of cells treated by vehicle control (Ctrl) or FKA at half-maximal inhibitory concentration in each cell lines with and without the DEAB (ALDH inhibitor) were shown. Statistical analysis of ALDH activity after treatment of a gradient-dose FKA in both cell lines was shown on the right. ALDH activity was decreased in FKA treated group in a dose-dependent manner. (B) Representative pictures of spheres formation assay were shown on the left, and statistical analysis was shown on the right. FKA treatment of Hssy-II and Syo-1 cell lines reduced the number of sarcosphere in a dose-dependent manner. (C) Hssy-II cells were subcutaneously injected into the flank of SCID mice and randomized into two groups. Treatment of 0.5% w/v CMC or FKA (600 mg/kg per day) were implicated in two groups. The relative tumor volume growth from six independent xenografts after treatment was measured. (D) The relative tumor volume at last measurement was significantly reduced after FKA treatment compared to control (CMC). ($P = .026$). Statistical significance is indicated by $^{*}P < .05$,$^{**}P < .01$, $^{***}P < .001$. Column: mean; error bars: SD.

of p27 has been shown to activate glial stem cells via Notch signaling [27]. Skp2 downregulation by siRNA leads to a reduction in neurosphere formation in the presence of Jag1, suggesting that Skp2 is essential for Notch-mediated stemness in the central nervous system [27]. In SS, a survival analysis suggested that the lack of p27 is an independent negative prognostic factor for overall patient survival [28]. In human embryonic stem cells, overexpression of p27 reduces the capacity for self-renewal [19]. Mechanistically, p27 protein likely functions as a repressor of Twist1 gene expression by occupying the Twist1 promoter [19]. Therefore, loss of p27 leads to increased stemness and upregulation of Twist1. In our study, depletion of Skp2 either by genetic knockdown or by the neddylation inhibitor FKA led to a significant elevation of p27 protein, concomitant with a decrease in Twist1 and a corresponding decrease in TIC properties such as sarcosphere formation and ALDH. Together, these results suggest that inhibitors of the Skp2-p27 axis may have clinical utilities in SS by modulating stemness properties. Further investigations are needed to elucidate branch points within the Skp2-p27 axis to intervene to achieve maximal antitumoral activities while avoiding off-target effects.

The existence of TICs is regarded as a major cause of chemotherapy resistance and treatment failure in cancer. Recent studies suggest that TICs are enriched after chemotherapy because most chemotherapeutic drugs are only effective in killing the majority of cells within the bulk tumor mass while leaving the TIC subpopulation intact [29]. ALDH, an enzyme that protects cells from the toxic effects of reactive oxygen species, is considered a marker for TIC in many types of cancer, including breast, lung, and rhabdomyosarcoma [30–32]. Inhibitors of ALDH activity can serve to sensitize TICs to chemotherapeutic drugs. For example, treatment of colon cancer TICs with an ALDH inhibitor or siRNA has been shown to increase sensitivity to cyclophosphamide in xenograft models [33]. In our study, both ALDH levels and sphere-forming capacity of SS cells are negatively affected by Skp2 downregulation, suggesting that Skp2 serves to promote TIC properties in SS. Similarly, the treatment of SS cell lines with FKA also reduced the levels of Skp2 and ALDH. In addition, our *in vitro* data showed that FKA and doxorubicin exert a synergistic efficacy, thus implicating a role for Skp2 inhibitors in suppressing the TIC subpopulation in SS. Further studies using appropriate model systems are needed to establish the role for Skp2 inhibition in chemoresistant SS.

Interestingly, data extracted from the TCGA database (Supplementary Figure 1) reveal that high expression of Skp2 in a cohort of 206 soft tissue sarcoma samples, several of which are SS tumors, correlates with poor overall survival. This finding suggests that Skp2 may serve as a prognostic biomarker in soft tissue sarcoma and deserves further investigation. The clinical significance and predictive value of p27, on the other hand, are still unclear in SS. Kawauchi and colleagues performed a clinicopathologic analysis of 55 primary SS samples and found that low expression of p27 was an independent predictor of poor prognosis [28]. However, a study by Antonescu et al. failed to confirm that p27 expression is a predictive biomarker in SS [34]. These conflicting findings may reflect the complex relationship

between Skp2 and its target p27 and may point to other events such as protein phosphorylation states or chaperones that need further studies.

To the best of our knowledge, this study is the first to identify the F-box protein Skp2 as a potential therapeutic target for synovial sarcoma. Our findings revealed that advanced clinical stages of SS express higher levels of Skp2 and that genetic knockdown of Skp2 inhibits SS proliferation, invasion, and cancer stemness. These data form the basis of our hypothesis that conventional chemotherapies may not prevent relapses in SS if the TIC subpopulation is not appropriately targeted. Specifically, targeting the interactions of Skp2 with Twist1 and its ubiquitination target p27 might lead to strategies to overcome the stemness plasticity of SS. As such, combination trials of Skp2 inhibitors and conventional chemotherapeutic drugs in SS may be desirable.

Conflict of Interest Statement

The authors declare no conflict of interest.

Authors' Contributions

Conceptualization: J. W., K. S., D. W., D. L., R. G., E. S., R. Y., X. Z., H. Z., D. G., B. H.; methodology and analysis: J. W., K. S., E. D., A. S., S. Y., O. A., B. B., H. B., J. Z., H. Z.; investigation: J. W., K. S., J. T., D. W., D. L., R. G., E. S., R. Y., X. Z., H. Z., D. G., B. H.; writing: J. W., K. S., E. D., B. B., J. T., H. Z., B. H.

Acknowledgements

This work was supported by the Live for Others Foundation, Sarcoma Strong, Montefiore Medical Center (to B.H.), and the National Institutes of Health (R01CA193967 to X.Z.; R01CA230032 and R01201458 to H.Z. and E.S.)

Appendix A. Supplementary Data

Supplementary data to this article can be found online at https://doi.org/10.1016/j.tranon.2020.100809.

References

[1] A. Kawai, J. Woodruff, J.H. Healey, M.F. Brennan, C.R. Antonescu, M. Ladanyi, SYT-SSX gene fusion as a determinant of morphology and prognosis in synovial sarcoma, N. Engl. J. Med. 338 (3) (1998) 153–160.
[2] F.C. Eilber, M.F. Brennan, F.R. Eilber, J.J. Eckardt, S.R. Grobmyer, E. Riedel, C. Forscher, R.G. Maki, S. Singer, Chemotherapy is associated with improved survival in adult patients with primary extremity synovial sarcoma, Ann. Surg. 246 (1) (2007) 105–113.
[3] M. El Beaino, D.M. Araujo, A.J. Lazar, P.P. Lin, Synovial sarcoma: advances in diagnosis and treatment identification of new biologic targets to improve multimodal therapy, Ann. Surg. Oncol. 24 (8) (2017) 2145–2154.
[4] P. Bergh, J.M. Meis-Kindblom, F. Gherlinzoni, O. Berlin, P. Bacchini, F. Bertoni, B. Gunterberg, L.G. Kindblom, Synovial sarcoma: identification of low and high risk groups, Cancer 85 (12) (1999) 2596–2607.
[5] D. Ruan, J. He, C.F. Li, H.J. Lee, J. Liu, H.K. Lin, C.H. Chan, Skp2 deficiency restricts the progression and stem cell features of castration-resistant prostate cancer by destabilizing Twist, Oncogene 36 (30) (2017) 4299–4310.
[6] C.H. Chan, J.K. Morrow, S. Zhang, H.K. Lin, Skp2: a dream target in the coming age of cancer therapy, Cell Cycle 13 (5) (2014) 679–680.
[7] M. Gstaiger, R. Jordan, M. Lim, C. Catzavelos, J. Mestan, J. Slingerland, W. Krek, Skp2 is oncogenic and overexpressed in human cancers, Proc. Natl. Acad. Sci. U. S. A. 98 (9) (2001) 5043–5048.
[8] Y. Liang, X. Hou, Q. Cui, T.B. Kang, J.H. Fu, L.J. Zhang, R.Z. Luo, J.H. He, Y.X. Zeng, H. X. Yang, Skp2 expression unfavorably impacts survival in resectable esophageal squamous cell carcinoma, J. Transl. Med. 10 (2012) 73.
[9] J. Wang, Y. Huang, Z. Guan, J.L. Zhang, H.K. Su, W. Zhang, C.F. Yue, M. Yan, S. Guan, Q.Q. Liu, E3-ligase Skp2 predicts poor prognosis and maintains cancer stem cell pool in nasopharyngeal carcinoma, Oncotarget 5 (14) (2014) 5591–5601.
[10] Y. Zhang, Y.S. Zvi, B. Batko, N. Zaphiros, E.F. O'Donnell, J. Wang, K. Sato, R. Yang, D.S. Geller, P. Koirala, et al., Down-regulation of Skp2 expression inhibits invasion and lung metastasis in osteosarcoma, Sci. Rep. 8 (1) (2018) 14294.
[11] N. Naka, S. Takenaka, N. Araki, T. Miwa, N. Hashimoto, K. Yoshioka, S. Joyama, K. Hamada, Y. Tsukamoto, Y. Tomita, et al., Synovial sarcoma is a stem cell malignancy, Stem cells (Dayton, Ohio) 28 (7) (2010) 1119–1131.
[12] B. Lohberger, B. Rinner, N. Stuendl, M. Absenger, B. Liegl-Atzwanger, S.M. Walzer, R. Windhager, A. Leithner, Aldehyde dehydrogenase 1, a potential marker for cancer stem cells in human sarcoma, PLoS One 7 (8) (2012), e43664. .
[13] K.W. Lee, N.K. Lee, S. Ham, T.Y. Roh, S.H. Kim, Twist1 is essential in maintaining mesenchymal state and tumor-initiating properties in synovial sarcoma, Cancer Lett. 343 (1) (2014) 62–73.
[14] C. Wu, Q. Wei, V. Utomo, P. Nadesan, H. Whetstone, R. Kandel, J.S. Wunder, B.A. Alman, Side population cells isolated from mesenchymal neoplasms have tumor initiating potential, Cancer Res. 67 (17) (2007) 8216–8222.
[15] A. Martin, A. Cano, Tumorigenesis: Twist1 links EMT to self-renewal, Nat. Cell Biol. 12 (10) (2010) 924–925.
[16] Phinney DG. Twist, epithelial-to-mesenchymal transition, and stem cells. Stem cells (Dayton, Ohio). 2011;29(1):3–4.
[17] K.W. Lee, J.H. Kim, S. Han, C.O. Sung, I.G. Do, Y.H. Ko, S.H. Um, S.H. Kim, Twist1 is an independent prognostic factor of esophageal squamous cell carcinoma and associated with its epithelial-mesenchymal transition, Ann. Surg. Oncol. 19 (1) (2012) 326–335.
[18] T. Kimura, L. Wang, K. Tabu, M. Tsuda, M. Tanino, A. Maekawa, H. Nishihara, H. Hiraga, T. Taga, Y. Oda, et al., Identification and analysis of CXCR4-positive synovial sarcoma-initiating cells, Oncogene 35 (30) (2016) 3932–3943.
[19] C. Menchon, M.J. Edel, J.C. Izpisua Belmonte, The cell cycle inhibitor p27Kip(1) controls self-renewal and pluripotency of human embryonic stem cells by regulating the cell cycle, Brachyury and Twist. Cell Cycle. 10 (9) (2011) 1435–1447.
[20] S. Simeckova, Z. Kahounova, R. Fedr, J. Remsik, E. Slabakova, T. Suchankova, J. Prochazkova, J. Bouchal, G. Kharaishvili, M. Kral, et al., High Skp2 expression is associated with a mesenchymal phenotype and increased tumorigenic potential of prostate cancer cells, Sci. Rep. 9 (1) (2019) 5695.
[21] K. Shigemasa, L. Gu, T.J. O'Brien, K. Ohama, Skp2 overexpression is a prognostic factor in patients with ovarian adenocarcinoma, Clinical cancer research : an official journal of the American Association for Cancer Research. 9 (5) (2003) 1756–1763.
[22] T.C. Chou, Theoretical basis, experimental design, and computerized simulation of synergism and antagonism in drug combination studies, Pharmacol. Rev. 58 (3) (2006) 621–681.
[23] H. Zhao, Z. Lu, F. Bauzon, H. Fu, J. Cui, J. Locker, L. Zhu, p27T187A knockin identifies Skp2/Cks1 pocket inhibitors for advanced prostate cancer, Oncogene 36 (1) (2017) 60–70.
[24] X. Li, N.N. Yokoyama, S. Zhang, L. Ding, H.M. Liu, M.B. Lilly, D. Mercola, X. Zi, Flavokawain A induces deNEDDylation and Skp2 degradation leading to inhibition of tumorigenesis and cancer progression in the TRAMP transgenic mouse model, Oncotarget 6 (39) (2015) 41809–41824.
[25] J. Yang, S.A. Mani, J.L. Donaher, S. Ramaswamy, R.A. Itzykson, C. Come, P. Savagner, I. Gitelman, A. Richardson, R.A. Weinberg, Twist, a master regulator of morphogenesis, plays an essential role in tumor metastasis, Cell 117 (7) (2004) 927–939.
[26] S. Piccinin, E. Tonin, S. Sessa, S. Demontis, S. Rossi, L. Pecciarini, L. Zanatta, F. Pivetta, A. Grizzo, M. Sonego, et al., A "twist box" code of p53 inactivation: twist box: p53 interaction promotes p53 degradation, Cancer Cell 22 (3) (2012) 404–415.
[27] C.B. Del Debbio, Q. Mir, S. Parameswaran, S. Mathews, X. Xia, L. Zheng, A.J. Neville, I. Ahmad, Notch signaling activates stem cell properties of Muller glia through transcriptional regulation and Skp2-mediated degradation of p27Kip1, PLoS One 11 (3) (2016), e0152025. .
[28] S. Kawauchi, Y. Goto, X.P. Liu, T. Furuya, A. Oga, Y. Oda, M. Tsuneyoshi, K. Ihara, K. Sasaki, Low expression of p27(Kip1), a cyclin-dependent kinase inhibitor, is a marker of poor prognosis in synovial sarcoma, Cancer 91 (5) (2001) 1005–1012.
[29] M.R. Alison, W.R. Lin, S.M. Lim, L.J. Nicholson, Cancer stem cells: in the line of fire, Cancer Treat. Rev. 38 (6) (2012) 589–598.
[30] K. Nakahata, S. Uehara, S. Nishikawa, M. Kawatsu, M. Zenitani, T. Oue, H. Okuyama, Aldehyde dehydrogenase 1 (ALDH1) is a potential marker for cancer stem cells in embryonal rhabdomyosarcoma, PLoS One 10 (4) (2015), e0125454. .
[31] F. Jiang, Q. Qiu, A. Khanna, N.W. Todd, J. Deepak, L. Xing, H. Wang, Z. Liu, Y. Su, S.A. Stass, et al., Aldehyde dehydrogenase 1 is a tumor stem cell-associated marker in lung cancer, Molecular cancer research : MCR. 7 (3) (2009) 330–338.
[32] C. Ginestier, M.H. Hur, E. Charafe-Jauffret, F. Monville, J. Dutcher, M. Brown, J. Jacquemier, P. Viens, C.G. Kleer, S. Liu, et al., ALDH1 is a marker of normal and malignant human mammary stem cells and a predictor of poor clinical outcome, Cell Stem Cell 1 (5) (2007) 555–567.
[33] S.J. Dylla, L. Beviglia, I.K. Park, C. Chartier, J. Raval, L. Ngan, K. Pickell, J. Aguilar, S. Lazetic, S. Smith-Berdan, et al., Colorectal cancer stem cells are enriched in xenogeneic tumors following chemotherapy, PLoS One 3 (6) (2008), e2428. .
[34] C.R. Antonescu, D.H. Leung, M. Dudas, M. Ladanyi, M. Brennan, J.M. Woodruff, C. Cordon-Cardo, Alterations of cell cycle regulators in localized synovial sarcoma: a multifactorial study with prognostic implications, Am. J. Pathol. 156 (3) (2000) 977–983.